

Phase diagram of the $t - t'$ Hubbard model taking into account spin-spiral waves and phase separation at finite temperatures

A.K. Arzhnikov^{1,*} and A.G. Groshev^{1,†}

¹*Physical-Technical Institute, Ural Division of RAS, Izhevsk, Russia*

(Dated: October 30, 2019)

The effect of temperature on the magnetic phase separation and the parameters of spin-spiral waves (SSW) is studied using a two-dimensional (2D) single-band $t - t'$ Hubbard model and the Hubbard-Stratonovich transformation. Both commensurate (antiferromagnetic (AF)) and incommensurate (helical) magnetic phases are considered. It is shown that the temperature significantly affects the collinear and helical magnetic phases. With an increase in the temperature, the phase-separation (PS) regions (AF+[Q, Q]), ($[Q, Q] + [Q, \pi]$) get substantially reduced but new regions ($[Q_1, \pi] + [Q_2, \pi]$), (AF+[Q, π]) arise. The results are used for the interpretation of the magnetic properties of cuprates.

PACS numbers: 75.10.Lp, 71.10.Fd, 71.10.Hf, 75.30.Fv

The discovery, in the late 1980s, of high-temperature superconductivity giving rise to new extensive studies of the phenomenon of superconductivity, has also regenerated a vivid interest in quantum low-dimensional magnetism. At present most researchers are inclined to believe that magnetic interactions are responsible in great part (if not completely) for the high-temperature superconductivity. Apparently, the high-temperature pseudogap observed in superconductors is also connected with magnetism, rather than with the Cooper pairs [1]. Theoretical description of magnetism in these systems is still far from complete. As is shown experimentally [2], the itinerant magnetism should enter as an essential component into theoretical models. Of great importance therewith is the two-dimensionality [3, 4]. The authors of paper [5] have studied the ground-state phase diagram of the 2D single-band Hubbard model. The calculations were performed in the framework of the mean field approximation with consideration of both commensurate (ferromagnetic and AF) and incommensurate (SSW) magnetic states. The results obtained made it possible to explain some peculiarities of the behavior of superconducting cuprates, and clarified the role of spatial magnetic phase separation (PS). Further investigation of the model at finite temperatures [6] has shown the necessity of taking into account the next-nearest-neighbor hopping, and revealed a significant influence of thermodynamic fluctuations on the boundaries of PS regions.

In this paper we consider the 2D single-band Hubbard model at finite temperatures with allowance for the next-nearest-neighbor hopping. Note a controversial point that arises in studying the 2D models. It is related to the well known statement that magnetic order is lacking in 2D systems at finite temperatures (except for the Ising-type models). As a rule, the researchers which use the 2D Hubbard model for describing cuprates assume that the weak magnetic coupling between the Cu layers suppresses anomalous growth of transverse magnetic fluctuations and stabilizes the order, ensuring a quasi-

two-dimensional behavior of the magnetic characteristics. However there may be an alternative mechanism of suppressing the anomalous growth of magnetic fluctuations through the charge degree of freedom and the volume Coulomb interaction. In this case one can speak of a 2D magnetic subsystem. The problem of the existence of 2D magnetism is similar to that of the 2D crystals in which the anomalous growth of lattice fluctuations is suppressed owing to strong anharmonicity of the longitudinal and transverse lattice vibrations [7]. In view of the above, in this work we use a special approximation which makes it possible to prevent anomalous growth of magnetic fluctuations and stabilize the magnetic order of the 2D model, leaving the question of the existence of 2D ordered structures unsettled. It should be noted that the results of such approximations are useful even in the absence of long-range magnetic order, as they may be used for the description of the dominant thermodynamical magnetic fluctuations at fixed temperatures. Another controversial point of our study is the choice of possible incommensurate magnetic structures. We have restricted our consideration to the helical magnetic phases (SSW), leaving aside the collinear spin-density waves (SDW). Usually, the findings obtained in neutron experiments give no possibility to distinguish between SSW and SDW (see, e.g., [8–11], except in a few cases such as the spin-polarized experiments on Fe-As monocrystals [12] where the existence of SSW has been established unambiguously. Ab initio calculations show that SSW may be realized in many systems on basis of the transition metals [13]. A direct comparison of the SSW and SDW energies within the 2D Hubbard model shows that in some cases the SDW are energetically preferable [14]. At the same time the obtained charge redistribution over the sites in SDW is too large, and the Coulomb interaction, not accounted for in the model, should increase the SDW energy, making these states unfavorable.

MODEL

We adopt the Hamiltonian of the Hubbard model on the squared lattice $\hat{H} = \hat{H}_0 + \hat{H}_{int}$,

$$\hat{H}_0 = \sum_{ijs} t_{ij} \hat{c}_{is}^+ \hat{c}_{js}, \quad \hat{H}_{int} = U \sum_j \hat{n}_{j\uparrow} \hat{n}_{j\downarrow}, \quad (1)$$

where $t_{ij} = -t$ for the nearest-neighbor sites i, j , $t_{ij} = t'$ for the next-nearest neighbors, $\hat{n}_{js} = \hat{c}_{js}^+ \hat{c}_{js}$ is the electrons number operator with spin projection $s = \uparrow, \downarrow$ on site j , \hat{c}_{js}^+ (\hat{c}_{js}) is a creation (annihilation) electronic operator with spin projection s on site j . U denotes the interatomic Coulomb interaction on site.

We consider the helical-type magnetic structures corresponding to the magnetization vector uniformly rotating in the polarization plane when moving from one site to another. This magnetic structure is characterized by the magnitude and direction of the wave vector $Q = [Q_x, Q_y]$. Generally, the wave vector Q does not coincide with a reciprocal lattice vector and turns out to be incommensurate [5, 6]. The superposition of the helical wave and the ferromagnetic component perpendicular to the polarization plane has a large energy [15] and it is not considered here.

The thermal properties of the system are determined by the partition function of the grand canonical ensemble

$$Z = Tr \left[T_\tau \exp \left\{ - \int_0^\beta \hat{H}(\tau) d\tau \right\} \right]. \quad (2)$$

Here the symbol Tr denotes summation over the complete set of quantum states, T_τ denotes the time ordering operator, $\beta = 1/k_B T$ denotes the inverse temperature, $\hat{H}(\tau)$ is the $\hat{H} - \mu \hat{n}$ operator in the interaction representation where μ and \hat{n} are the chemical potential and the total electron number operator, respectively.

Partition function (2) for the many-particle problem is transformed into that of the single-particle problem with time-dependent fictitious fields, by means of the functional integral method through the use Hubbard-Stratonovich transformation [16]. To reproduce the results of the generalized Hartree-Fock approximation at the ground state [5, 6] we need to use the two-field functional integral method in the static approximation [17] introducing the spin and charge auxiliary fictitious fields, \mathbf{v}_j and ζ_j . In addition, we adopted the saddle point approximation for the charge auxiliary fictitious field ζ_j what corresponds to the replacement of the ζ_j by its value $\zeta_j^0(\mathbf{v}_j)$ at the saddle point. Using $\zeta_j^0(\mathbf{v}_j)$, we minimize the thermodynamic potential at the fixed configuration \mathbf{v}_j , but neglect the charge fluctuations. In this work, we take into account only the longitudinal spin fluctuations specifying the direction of the spin auxiliary fictitious field \mathbf{v}_j parallel to the magnetization vector \mathbf{m}_j at each site.

The partition function is expressed by the mean field approximation for the single-particle Green function

$\hat{G}(z) = [z - \hat{\mathcal{H}}_{MF}]^{-1}$ [18, 19], where $\hat{\mathcal{H}}_{MF}$ is the mean field approximation for the Hubbard Hamiltonian (1). Finally, we introduce the self-energy of electron in the effective medium Σ , which is determined by the average with respect to the amplitude of spin fictitious field v Green function $\tilde{G} = \langle [1 - GV(v)]^{-1} G \rangle$. The effective self-energy Σ and \tilde{G} are found using the self-consistent matrix equation in the single-site coherent potential approximation

$$\tilde{G}(z) = \langle [1 - GV(v)]^{-1} G \rangle = G(z - \Sigma). \quad (3)$$

After introducing these approximations, the partition function is represented in the form of an integral over the amplitude of spin fictitious field v

$$Z = \exp \{ -\beta(\Omega[\Sigma] + \Delta\Omega) \}, \quad (4)$$

$$\begin{aligned} \Omega[\Sigma] &= \Omega_{MF} - \frac{1}{\beta} \sum_n \ln \det [1 + \Sigma(i\omega_n) \tilde{G}(i\omega_n)], \\ \Delta\Omega &= -\frac{1}{\beta} \ln \int dv \exp \{ -\beta \Delta\Omega(v) \}, \\ \Delta\Omega(v) &= \frac{1}{\beta} \sum_n \ln \det [1 - \tilde{G}(i\omega_n)(V(v) - \Sigma(i\omega_n))] \\ &\quad + U [v^2 + \zeta^2(v)]. \end{aligned}$$

Here $\Omega[\Sigma]$ is the thermodynamic potential for the effective medium, which is determined by the effective self-energy Σ , and $\Delta\Omega$ is the fluctuating part of the thermodynamic potential, $\Omega_{MF} = -1/\beta \ln Tr \exp [-\beta(\hat{\mathcal{H}}_{MF} - \mu \hat{n})]$ is the mean field approximation for the thermodynamical potential of electrons, $\omega_n = \pi(2n + 1)/\beta$ are the Matsubara frequencies for the Fermi particles. For brevity, site subscript in (4) is omitted.

We mentioned earlier that the ground state in this approximation is the Hartree-Fock state, which is formally validated in the limit of the small parameter U/t . In our theoretical approach, the analysis of the approximations in terms of the small parameter at nonzero temperature is an extremely complicated problem, which is still unsolved. Nevertheless, the static approximation is justified since we are not studying the superconducting properties of our systems and the strong correlations in the chosen range of parameters at the electron density close to unity are not very significant. This is confirmed by comparison of our results [5] with those obtained by the dynamical cluster methods [20].

In spite of the aforementioned essential approximations, further analysis of expression (4) is possible only by using numerical methods. The self-consistent solution to (3) and (4) allows us to calculate all magnetic properties of our system under the condition that the magnetic state with the minimum thermodynamic potential is chosen.

RESULTS

All calculations were carried out at $U/t = 4.8$, $t'/t = 0.2$. For these values various magnetic phases are realized [5], and the characteristics of the electron states of superconducting cuprates ($La_{(2-x)}Sr_xCuO_4$) [21] may be described well enough. We restricted ourselves to the electron concentrations less than unity, because in a wide range of larger concentrations the system exhibits a stable AF ordering [5]. Figure 1 presents the $T - n$ phase diagram (hereafter we shall use a dimensionless temperature $T \rightarrow k_B T/t$). Thick solid lines correspond to the phase transitions between states with different magnetic order. The phase transition from the ordered magnetic state to a paramagnet (P) is a second-order transition, all the other are first-order transitions. This is well illustrated by the dependence of chemical potential on the electron concentration at $T = 0.02$ Fig. 2 which exhibits a inflection when passing from AF to the diagonal $[Q, Q]$ phase, and from $[Q, Q]$ to the parallel $[Q, \pi]$ phase. Instability of the chemical potential (negative derivative with respect to concentration) results in spatial magnetic phase separation (PS) whose boundaries are determined by the Maxwell rule:

$$\int_{n_1}^{n_2} [\mu(n_1) - \mu(n)] dn = 0, \quad (5)$$

where n_1 and n_2 are the boundaries of the PS region. A comparison of the PS region boundaries at zero and finite temperatures shows that with increasing temperature the PS regions narrow down, being replaced by homogeneous states. Besides there arise three new PS regions: ($[Q_1, \pi] + [Q_2, \pi]$), ($[Q, Q] + [Q, \pi]$), and (AF + $[Q, \pi]$) which were lacking at zero temperature. The characteristics of the magnetic phases and their partial ratios inside the PS regions are completely determined by their values at the boundaries of these regions. Figures 3, 4, 5, 6 present the parameters of spiral magnetic structures at the PS boundaries (AF + $[Q, Q]$), ($[Q, Q] + [Q, \pi]$), ($[Q_1, \pi] + [Q_2, \pi]$), and (AF + $[Q, \pi]$). These plots may be used to determine the mean local magnetization at site $\langle m \rangle$, the mean absolute magnitude of local magnetization $\langle |m| \rangle$, the spiral wave vector Q , and the partial phase ratio for any point inside the PS region.

Of interest is a rather strong T dependence of Q in the phase mixture (AF + $[Q, Q]$), see Fig. 3. In experiments on cuprates close to half filling a region, generally referred to as "spin glass" (SG), is observed [4]. The PS (AF + $[Q, Q]$) with a strong temperature dependence of vector Q found in our study can be easily associated with the experimentally observed SG region. Note that the ratio between the temperatures T_N and T_g corresponding to the $P \rightarrow AF$ and $AF \rightarrow SG$ transitions, respectively, for $n = 0.98$ is approximately equal to 12 [11], which agrees with the ratio of temperatures T_N and T_{PS} for

the $P \rightarrow AF$ and $AF \rightarrow (AF + [Q, Q])$ transitions, respectively, in our calculation Fig. 1. Recall that the calculated absolute values of the transition temperatures are overestimated because of the model and computational approximations made (see Section 1). The distinctive feature of the PS regions ($[Q_1, \pi] + [Q_2, \pi]$) Fig. 5 and (AF + $[Q, \pi]$) Fig. 6 consists in a large difference between the mean local magnetic moments in the phase mixture, the absolute magnitudes of local magnetic moments being approximately equal. At high temperatures this fact can be interpreted as the effect of long-lived fluctuations against a paramagnetic-state background [3]. Besides, the superparamagnetic behavior experimentally observed in chemically homogeneous Fe-Al alloys at high temperatures [22] is easily explained when taking into account the possibility of spatial magnetic separation between SSW and the ferrimagnetic phase. Note that low-temperature neutron experiments have revealed in these alloys the existence of SDW [23] the parameters of which are fairly well described in ab initio calculations using SSW [22, 24].

The temperature and concentrational behavior of the PS region ($[Q, Q] + [Q, \pi]$) reproduces two significant experimental facts [10]. A decrease in the number of electrons results in the following sequence of transitions: $[Q, Q] \rightarrow ([Q, Q] + [Q, \pi]) \rightarrow [Q, \pi]$, and an increase in the temperature gives rise to the transition ($[Q, Q] + [Q, \pi] \rightarrow [Q, \pi]$, see Figs. 1, 4. It should be noted that quantitative agreement with the experimental concentrations of the transitions cannot be expected in our calculations, as they are extremely sensitive to the parameters U/t and t'/t . An insignificant decrease in U/t from 4.8 leads to a considerable shift of these transitions towards concentrations close to unity, and at $U/t < 4$ the concentrational transition connected with the $[Q, Q]$ phase totally disappears, see [5].

The authors of paper [5] have pointed out the proportional dependence of the wave vector on the electron concentration, which is in agreement with the experiment [10] and can be easily interpreted in terms of the spin-spiral structure formation. At finite temperatures this dependence is retained, see, e.g. Fig. 2. Moreover, in the considered range of concentrations n , a general tendency for an increase in the SSW wave vector with temperature is observed. This is true both for each of the PS phases Figs. 3-6 and for the homogeneous states Fig. 7. However note that in the PS region the mean wave vector can diminish with increasing temperature. This is the case, for example, in the PS ($[Q_1, \pi] + [Q_2, \pi]$) because of a change in the partial phase ratio, namely, a decrease with increasing temperature in the portion of the phase with larger wave vector Fig. 5. Of particular interest is the temperature transition metal-insulator near the concentration equal to unity.

Figures 8 and 9 show the density of states for the AF and $[Q, Q]$ phases in the PS (AF + $[Q, Q]$) region at temperatures 0.02 and 0.002. It is seen that for $T = 0.02$ all

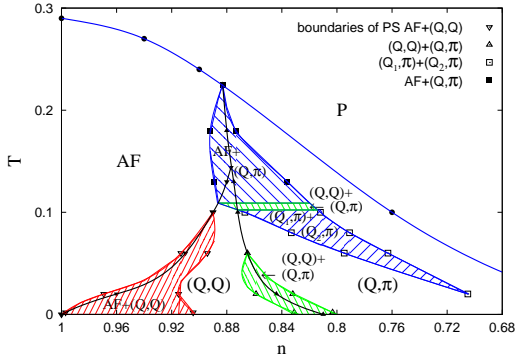


Figure 1: (Color online) Magnetic phase diagram at $U/t = 4.8$ and $t'/t = 0.2$. Blue bold line denote the Neel temperature (second-order phase transition), black bold lines denote first-order phase transitions calculated without regard for PS, shaded areas denote PS regions.

the phases are metallic, and AF phase may be considered as a conductor, since it has a lower electron density at the Fermi level as compared to the $[Q, Q]$ phase Fig. 8(a). With decreasing temperature the AF phase actually becomes insulator, and the conductivity of the $[Q, Q]$ phase increases Fig. 9(a). The metal-insulator transition experienced by the AF phase is a Slater-type transition [25]. The total density of states for temperatures 0.02 and 0.002, and concentration $n = 0.96$ is shown in Fig. 8(b) and Fig. 9(b). In both cases the total density of electron states at the Fermi level is different from zero. It is obvious however that at low temperature the system is practically an insulator, because at this temperature and concentration the portion of the AF phase relative to the $[Q, Q]$ phase exceeds 1/2 (the percolation threshold in the 2D case being equal to 1/2). Thus our system will undergo a metal-insulator transition in the concentration range $1 \div 0.95$, but this is a Slater-type transition of percolation character. We did not account for the strong electron correlations which could modify the boundaries and features of the region of the transition described. It is also evident that with a decrease in the electron concentration (hole doping) the role of correlations substantially grows. The Mott transitions induced by the strong correlations in optimally doped and overdoped cuprate regions have been considered in detail in the review [26].

CONCLUSION

Thus, based on 2D Hubbard model, we have studied the formation of helical waves (SSW) and the magnetic PS at finite temperatures. The calculated $T - n$ phase diagram Fig. 1 shows that the PS regions existing at $T = 0$ with increasing temperature get much narrower,

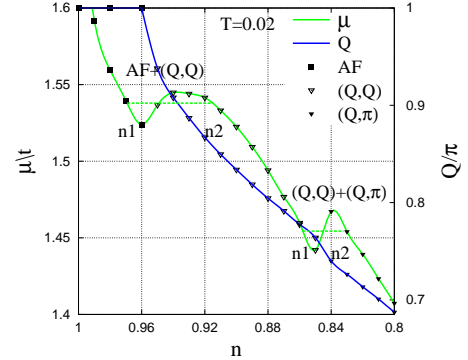


Figure 2: (Color online) Chemical potential μ (left axis) and wave vector Q (right axis) versus the electron density n at $U/t = 4.8$ and $t'/t = 0.2$. Dashed lines denote n dependence of the μ in the PS regions.

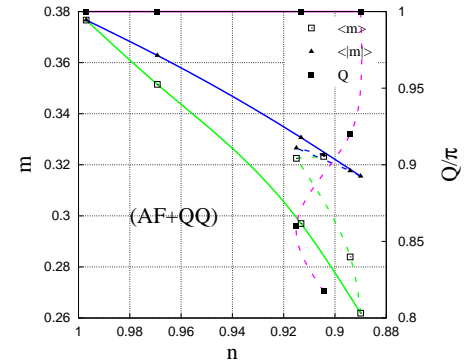


Figure 3: (Color online) Electron number dependence of the average local magnetic moment $\langle m \rangle$ and its absolute value $\langle |m| \rangle$ (left axis), wave vector Q (right axis) along the boundary of AF + $[Q, Q]$ PS region at $U/t = 4.8$ and $t'/t = 0.2$. Dashed lines - $[Q, Q]$ phase, bold lines - AF.

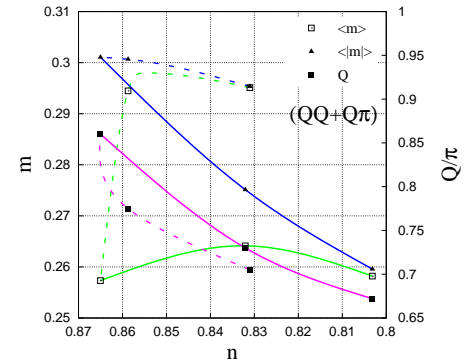


Figure 4: (Color online) $[Q, Q] + [Q, \pi]$ PS region. Dashed lines - $[Q, Q]$ phase, bold lines - $[Q, \pi]$. Notations are the same as in Fig. 3.

and there arise new PS areas with different symmetry of

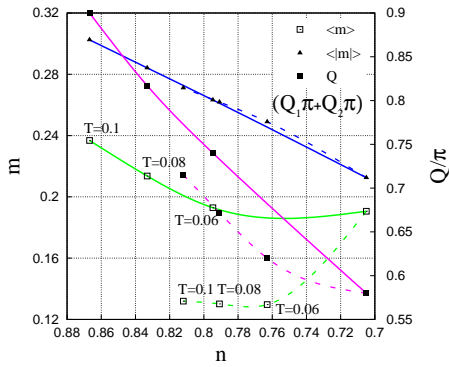


Figure 5: (Color online) $[Q_1, \pi] + [Q_2, \pi]$ PS region. Dashed lines - top boundary with $[Q, \pi]$ phase, bold lines - lower boundary with $[Q, \pi]$ phase. Notations are the same as in Fig. 3.

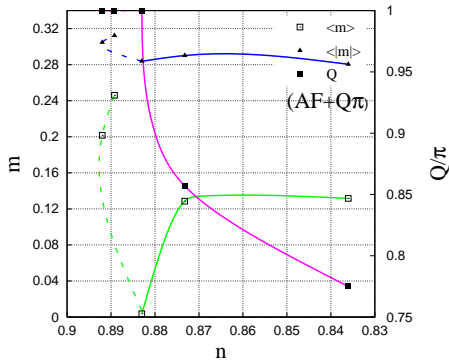


Figure 6: (Color online) AF + $[Q, \pi]$ PS region. Dashed lines - AF, bold lines - $[Q, \pi]$. Notations are the same as in Fig. 3.

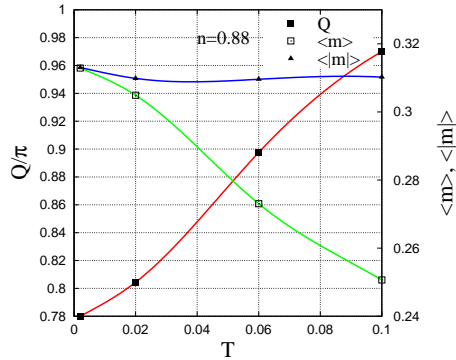


Figure 7: (Color online) Temperature dependence of the wave vector Q (left axis), average local magnetic moment $\langle m \rangle$ and its magnitude $\langle |m| \rangle$ (right axis) at $U/t = 4.8$, $t'/t = 0.2$ and $n = 0.88$.

the wave vectors SSW. The behavior of the wave vectors, mean local magnetic moments, and mean absolute magnitudes of the local moments is described for both

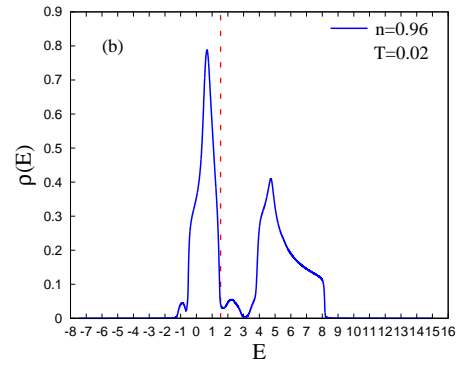
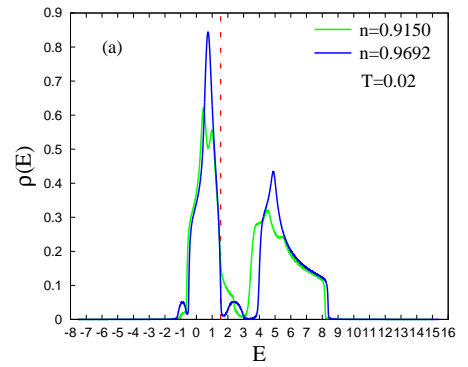


Figure 8: (Color online) Electron density of states EDS in the AF + $[Q, Q]$ PS region. (a) Portion EDS on the boundaries of PS at $T = 0.02$. (b) Total EDS at $T = 0.02$ and $n = 0.96$. Dashed line - Fermi level $U/t = 4.8$, $t'/t = 0.2$

the homogeneous SSW states and the phases forming the PS region. It is shown that the mean local magnetic moments of different phases inside the PS region may considerably differ in magnitude and temperature behavior. The wave vectors for all SSW increase with temperature. The proportionality of the SSW wave vectors to the number of electrons (holes) is retained in a wide range of temperatures.

Taking account of the model and mathematical approximations made, the results obtained may be used to describe quasi-two-dimensional systems or the parameters of thermal magnetic fluctuations in the range of electron concentrations and temperatures where the effect of the strong correlations and system dynamics is not too significant.

A comparison of the results obtained with the available experimental data for high-temperature compounds $La_{(2-x)}Sr_xCuO_4$ shows a good semiquantitative agreement as to the behavior of the magnetic characteristics in the half-filling region with small hole concentration. The ratio between the temperatures T_N (P \rightarrow AF transition) and T_g (AF \rightarrow "spin glass" transition) at $n = 0.98$ approximates to 12 [11], which agrees with the ratio of temperatures T_N and T_{PS} for the P \rightarrow AF and AF \rightarrow (AF + $[Q, Q]$) transition, respectively, ob-

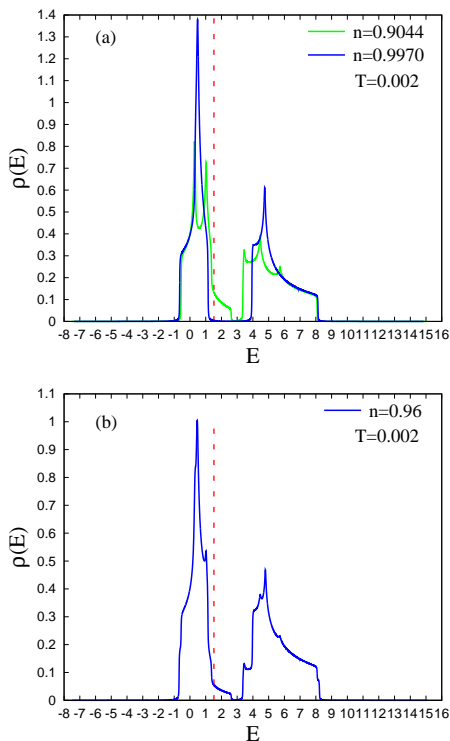


Figure 9: (Color online) (a) $T = 0.002$, $n = 0.9044$ and $n = 0.9970$. (b) $T = 0.002$ and $n = 0.96$. Notations are the same as in Fig. 8.

tained in our calculation. The presence of the PS region ($[Q, Q] + [Q, \pi]$), the sequence of transitions $[Q, Q] \rightarrow ([Q, Q] + [Q, \pi]) \rightarrow [Q, \pi]$ occurring with increasing concentration, and $([Q, Q] + [Q, \pi]) \rightarrow [Q, \pi]$ taking place with increasing temperature coincide with the PS region ($[Q, Q] + [Q, \pi]$) and the transition sequences observed experimentally [10].

Taking into account the possibility of a great difference in the mean local magnetic moment between the phases forming the PS region, one can explain the superparamagnetic behavior of chemically homogeneous alloys Fe-Al [22].

Obviously, allowance for the strong correlations and the system dynamics will affect the quantitative characteristics of the PS regions and the SSW parameters. However, as demonstrated by a comparison of T_N obtained in our calculations and in those performed within the dynamic cluster approximation (DCA) [20], the difference proves to be not very large.

This work was supported by the Russian Foundation for Basic Research (project No. 12-02-00632) and Ur Br RAS (project No. 12-U-2-1021).

* Electronic address: arzhnikof@bk.ru

† Electronic address: groshev_a.g@mail.ru

- [1] Rui-Hua He, M. Hashimoto, H. Karapetyan, J.D. Koralek, J.P. Hinton, J.P. Testaud, V. Nathan, Y. Yoshida, Hong Yao, K. Tanaka, W. Meevasana, R.G. Moore, D.H. Lu, S.-K. Mo, M. Ishikado, H. Eisaki, Z. Hussain, T.P. Devereaux, S.A. Kivelson, J. Orenstein, A. Kapitulnik, Z.-X. Shen, *Science* **331**, 1579 (2011).
- [2] Rui-Hua He, M. Fujita, M. Enoki, M. Hashimoto, S. Iikubo, S.-K. Mo, Hong Yao, T. Adachi, Y. Koike, Z. Hussain, Z.-X. Shen, and K. Yamada, *Phys. Rev. Lett.* **107**, 127002 (2011).
- [3] Shirane, G., Y. Endoh, R.J. Birgeneau, M.A. Kastner, Y. Hidaka, M. Oda, M. Suzuki, and T. Murakami, *Phys. Rev. Lett.* **59**, 1613 (1987).
- [4] M.A. Kastner, R.J. Birgeneau, G. Shirane, Y. Endoh, *Rev. Mod. Phys.* **70**, 897 (1998).
- [5] P.A. Igoshev, M.A. Timirgazin, A.A. Katanin, A.K. Arzhnikov, and V.Yu. Irkhin, *Phys. Rev. B* **81**, 094407 (2010).
- [6] A.K. Arzhnikov, A.G. Groshev, *JETP Lett.* **94**, 703 (2011).
- [7] A. Fasolino, J.H. Los and M.I. Katsnelson, *Nature* **78**, 2011 (2007).
- [8] K. Yamada, C.H. Lee, K. Kurahashi, J. Wada, S. Wakimoto, S. Ueki, H. Kimura, Y. Endoh, S. Hosoya, G. Shirane, R.J. Birgeneau, M. Greven, M.A. Kastner, and Y.J. Kim, *Phys. Rev. B* **57**, 6165 (1998).
- [9] M. Matsuda, M. Fujita, K. Yamada, R.J. Birgeneau, M.A. Kastner, H. Hiraka, Y. Endoh, S. Wakimoto and G. Shirane, *Phys. Rev. B* **62**, 9148 (2000).
- [10] M. Fujita, K. Yamada, H. Hiraka, P.M. Gehring, S.H. Lee, S. Wakimoto and G. Shirane, *Phys. Rev. B* **65**, 064505 (2002).
- [11] M. Matsuda, M. Fujita, K. Yamada, R.J. Birgeneau, Y. Endoh and G. Shirane, *Phys. Rev. B* **65**, 134515 (2002).
- [12] E.E. Rodriguez, C. Stock, K.L. Krycka, C.F. Majkrzak, P. Zajdel, K. Kirshenbaum, N.P. Butch, S.R. Saha, J. Paglione, and M.A. Green, *Phys. Rev. B* **83**, 134438 (2011).
- [13] R. Lizarraga, L. Nordstrom, L. Bergqvist, A. Bergman, E. Sjostedt, P. Mohn and O. Eriksson, *Phys. Rev. Lett.* **93**, 107205 (2004).
- [14] M.A. Timirgazin, A.K. Arzhnikov and A.V. Vedyayev, *Solid State Phenom.* **190**, 67 (2012).
- [15] M.A. Timirgazin and A.K. Arzhnikov, *Solid State Phenom.* **559**, 152 (2009).
- [16] Yu.A. Izyumov and Yu.N. Skryabin, *Statistical Mechanics of Magnetically Ordered Systems* (Nauka, Moscow, 1987; Springer-Verlag, New York, 1988).
- [17] R.F. Hassing, D.M. Esterling, *Phys. Rev. B* **7**, 432 (1973).
- [18] S.Q. Wang, W.E. Evenson, and J.R. Schrieffer, *Phys. Rev. Lett.* **23**, 92 (1969).
- [19] A.A. Abrikosov, L.P. Gor'kov, and I.E. Dzyaloshinskii, *Methods of Quantum Field Theory in Statistical Physics* (Fizmatlit, Moscow, 1963; Dover, New York, 1975).
- [20] T. Maier, M. Jarrell, T. Pruschke, M.H. Hettler, *Rev. Mod. Phys.* **77**, 1027, (2005).
- [21] A.I. Lichtenstein, M.I. Katsnelson, *Phys. Rev. B* **62**,

- R9283 (2000).
- [22] A.K. Arzhnikov, L.V. Dobysheva, M.A. Timirgazin, J. Magn. Magn. Mater. **320**, 1904 (2008).
- [23] D.R. Noakes, A.S. Arrott, M.G. Belk, S.C. Deevi, Q.Z. Huang, J.W. Lynn, R.D. Shull, D. Wu, Phys. Rev. Lett. **91**, 217201 (2003).
- [24] J. Bogner, W. Steiner, M. Reissner, P. Mohn, P. Blaha, K. Schwarz, R. Krachler, H. Ipser, B. Sepiol, Phys. Rev. B **58**, 14922 (1998).
- [25] M. Imada, A. Fujimori and Y. Tokura, Rev. Mod. Phys. **70**, 1039 (1998).
- [26] Patrick A. Lee, Naoto Nagaosa and Xiao-Gang Wen, Rev. Mod. Phys. **78**, 17 (2006).